

# Ribosome-Templated Azide–Alkyne Cycloadditions: Synthesis of Potent Macrolide Antibiotics by In Situ Click Chemistry

Ian Glassford,<sup>†</sup> Christiana N. Tejjaro,<sup>†</sup> Samer S. Daher,<sup>†</sup> Amy Weil,<sup>‡</sup> Meagan C. Small,<sup>§</sup> Shiv K. Redhu,<sup>||</sup> Dennis J. Colussi,<sup>#</sup> Marlene A. Jacobson,<sup>#</sup> Wayne E. Childers,<sup>#</sup> Bettina Buttaro,<sup>⊥</sup> Allen W. Nicholson,<sup>||</sup> Alexander D. MacKerell, Jr.,<sup>§</sup> Barry S. Cooperman,<sup>‡</sup> and Rodrigo B. Andrade<sup>\*,†</sup>

<sup>†</sup>Department of Chemistry, Temple University, Philadelphia, Pennsylvania 19122, United States

<sup>‡</sup>Department of Chemistry, University of Pennsylvania, Philadelphia, Pennsylvania 19104, United States

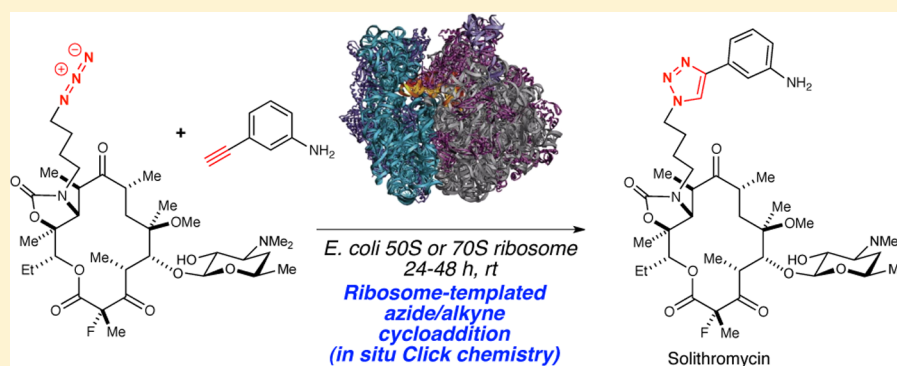
<sup>§</sup>Department of Pharmaceutical Sciences, School of Pharmacy, University of Maryland, Baltimore, Maryland 21201, United States

<sup>||</sup>Department of Biology, Temple University, Philadelphia, Pennsylvania 19122, United States

<sup>⊥</sup>Department of Microbiology and Immunology, Temple University School of Medicine, Philadelphia, Pennsylvania 19140, United States

<sup>#</sup>Moulder Center for Drug Discovery Research, Temple University School of Pharmacy, Philadelphia, Pennsylvania 19140, United States

## Supporting Information



**ABSTRACT:** Over half of all antibiotics target the bacterial ribosome—nature’s complex, 2.5 MDa nanomachine responsible for decoding mRNA and synthesizing proteins. Macrolide antibiotics, exemplified by erythromycin, bind the 50S subunit with nM affinity and inhibit protein synthesis by blocking the passage of nascent oligopeptides. Solithromycin (1), a third-generation semisynthetic macrolide discovered by combinatorial copper-catalyzed click chemistry, was synthesized in situ by incubating either *E. coli* 70S ribosomes or 50S subunits with macrolide-functionalized azide 2 and 3-ethynylaniline (3) precursors. The ribosome-templated in situ click method was expanded from a binary reaction (i.e., one azide and one alkyne) to a six-component reaction (i.e., azide 2 and five alkynes) and ultimately to a 16-component reaction (i.e., azide 2 and 15 alkynes). The extent of triazole formation correlated with ribosome affinity for the *anti* (1,4)-regioisomers as revealed by measured  $K_d$  values. Computational analysis using the site-identification by ligand competitive saturation (SILCS) approach indicated that the relative affinity of the ligands was associated with the alteration of macrolactone+desosamine-ribosome interactions caused by the different alkynes. Protein synthesis inhibition experiments confirmed the mechanism of action. Evaluation of the minimal inhibitory concentrations (MIC) quantified the potency of the in situ click products and demonstrated the efficacy of this method in the triaging and prioritization of potent antibiotics that target the bacterial ribosome. Cell viability assays in human fibroblasts confirmed 2 and four analogues with therapeutic indices for bactericidal activity over in vitro mammalian cytotoxicity as essentially identical to solithromycin (1).

## INTRODUCTION

Bacterial resistance to antibiotics is a formidable 21st century global public health threat.<sup>1–3</sup> If left unaddressed, we risk moving toward a “post-antibiotic” era.<sup>4</sup> While resistance is a natural consequence of antibiotic use (and abuse), the rate at which pathogenic bacteria have evaded multiple classes of drugs (including those of last resort) has markedly outpaced the rate

at which new drugs have been introduced. Macrolides are among the safest and most effective antibiotic classes. To date, three generations have been developed with only the lattermost targeting bacterial resistance.<sup>5,6</sup>

**Received:** December 12, 2015

**Published:** February 15, 2016

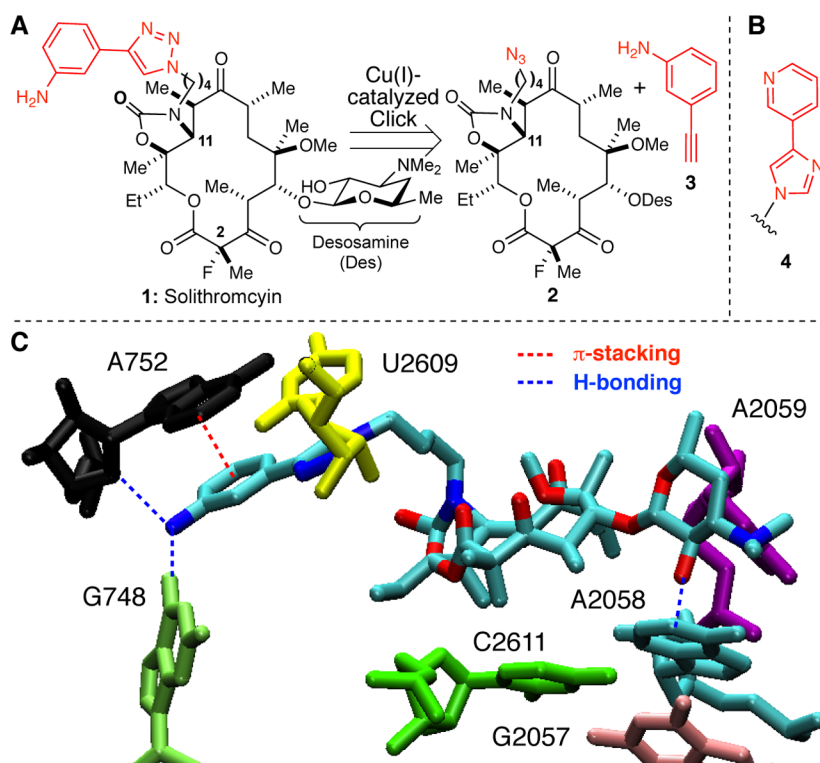


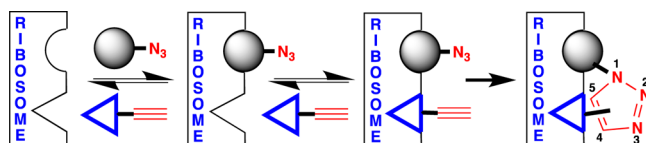
**Figure 1.** (A) Retrosynthetic analysis of solithromycin (1) yields azide 2 and aromatic alkyne 3. (B) Side-chain 4 from telithromycin. (C) Rendering of 1 and key 23S rRNA residues (Cate et al., PDB = 3ORB) using VMD.<sup>7</sup>

Solithromycin (1), one of the most potent macrolide antibiotics (Figure 1A), was prepared from the Cu(I)-catalyzed Huisgen [3 + 2] dipolar cycloaddition (i.e., “click”) reaction of azide 2 and 3-ethynylaniline (3).<sup>8</sup> Inspiration for 1 came from the erythromycin-derived ketolide telithromycin, which possesses a structurally related pyridyl-imidazole side-chain 4 (Figure 1B).<sup>9</sup>

Over half of all known antibiotics, including macrolides, target the bacterial ribosome.<sup>10</sup> Macrolides reversibly bind near the peptidyl transferase center of the 50S subunit with low nanomolar affinity and inhibit protein synthesis by blocking the passage of nascent oligopeptides.<sup>11,12</sup> The structure of the *E. coli* 70S ribosome-solithromycin (1) complex confirmed both the location and mode of binding.<sup>13</sup> Like other macrolides, 1 interacts with specific 23S rRNA residues via the macrolactone ring and desosamine sugar; moreover, the biaryl side-chain attached at N11 engages in  $\pi$ -stacking interactions with the A752-U2609 base pair and H-bonding with A752 and G748 (Figure 1C). Accordingly, we reasoned these molecular interactions could be leveraged in the ribosome-templated synthesis of solithromycin (1) from fragments 2 and 3 (Figure 1A); our target-guided synthesis strategy is illustrated in Scheme 1.<sup>14</sup>

Target-guided in situ click chemistry is predicated on the selective, proximal binding of azide- and alkyne-bearing fragments, which lowers the activation energy of irreversible 1,2,3-triazole ligation by colocalization.<sup>15</sup> Unlike the copper-catalyzed click reaction that exclusively provides the *anti* (1,4)-triazole<sup>16</sup> or the ruthenium-catalyzed variant that exclusively provides the *syn* (1,5)-triazole,<sup>17</sup> the in situ click process selectively provides the regioisomer that establishes optimal noncovalent interactions with the target (Scheme 1). Accordingly, the resultant cycloadduct is expected to have

#### Scheme 1. Ribosome-Templated In Situ Click Strategy for Antibiotic Synthesis<sup>a</sup>



<sup>a</sup>Sequential and proximal binding of azide- and alkyne-bearing fragments (e.g., 2 and 3, respectively) leads to irreversible *anti* (1,4)- and/or *syn* (1,5)-triazole formation by colocalization. The order in which the azide- and alkyne-functionalized fragments bind the target is determined by the individual binding affinities.

greater affinity for the target than the individual fragments.<sup>14</sup> In this regard, in situ click chemistry represents an extension of fragment-based drug design wherein the target directly participates in the synthesis of its own inhibitor<sup>18,19</sup> and has been successfully employed in the discovery of potent inhibitors for a number of targets, including acetylcholine esterase,<sup>20–23</sup> carbonic anhydrase,<sup>24</sup> HIV-protease,<sup>25</sup> Chitinase,<sup>26</sup> protein–protein interactions,<sup>27</sup> DNA-recognition,<sup>28</sup> EthR (a transcriptional regulator in *M. tuberculosis*),<sup>15,29,30</sup> and a toxic RNA, which was formed in cellulo.<sup>31</sup> Moreover, in situ click chemistry has been used extensively to create antibody-like protein capture agents.<sup>32–37</sup>

## RESULTS AND DISCUSSION

To test our hypothesis that bacterial ribosomes can template the Huisgen reaction, we synthesized azide 2 using known methods (see Supporting Information for details).<sup>38</sup> *Escherichia coli* 70S ribosomes, 50S and 30S ribosomal subunits were isolated as described.<sup>39</sup> After optimizing the concentrations of ribosomes, azide 2, and commercial 3-ethynylaniline (3) in

tris(hydroxymethyl)-aminomethane (Tris) buffer, we found that 5  $\mu\text{M}$  70S ribosomes or 50S subunits, 5  $\mu\text{M}$  azide, and 5 mM alkyne at rt for 24–48 h resulted in the formation of **1** and its *syn* (1,5)-regioisomer ( $\sim$ 2:1 ratio) in  $12 \pm 4$ -fold greater amounts than in the absence of 70S ribosome or 50S subunit (Figure 2). Analysis was performed on an Agilent 6520B Q-

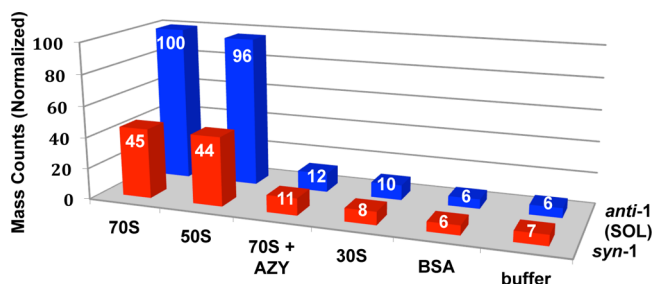


**Figure 2.** In situ click experiments with *E. coli* 70S ribosomes, 50S ribosomal subunits, 70S ribosomes with inhibitor azithromycin (AZY, 25  $\mu\text{M}$ ) and negative controls (30S ribosomal subunits, BSA, or buffer only). Mass counts (normalized) correspond to the combined *anti*-1 (solithromycin, SOL) and *syn*-1 regioisomer ions.

TOF LC–MS instrument wherein extracted ion chromatograms were used to locate and quantify the masses of interest (normalized to highest value).

Retention times of both *anti* (1,4)- and *syn* (1,5)-regioisomers were confirmed independently by chemical synthesis via thermal cycloaddition; moreover, solithromycin (**1**) was exclusively prepared by Cu(I)-catalysis.<sup>40</sup> Several lines of evidence strongly support the involvement of the large ribosomal subunit in the in situ click reaction: (1) in the absence of 70S ribosomes or 50S subunits (i.e., only buffer), there was  $12 \pm 4$ -fold less product formation, with the mass counts found corresponding to the thermal cycloaddition background reaction; (2) the 30S subunits, which do not possess a macrolide-binding site, also displayed mass counts similar to background; (3) the presence of ribosomal inhibitor azithromycin (AZY, 25  $\mu\text{M}$ ), which competes for the binding site with azide **2**, blocks 70S ribosome-dependent product formation; (4) replacing ribosomes with bovine serum albumin (BSA), a standard negative control used to rule out nonspecific binding, resulted in mass counts similar to those of the background cycloaddition; and finally, (5) the regioisomer ratio was  $\sim$ 1:1 in all control reactions (i.e., 30S, BSA, and buffer alone) and in the inhibition experiment with AZY, whereas in the presence of 70S ribosomes or 50S ribosomal subunits, the product ratio was 2:1 favoring **1**. Such selectivity is a hallmark of the orientational (i.e., regioselective) nature of target-guided in situ click chemistry.<sup>29</sup>

Having established the utility of in situ click chemistry in binary experiments (i.e., one azide, one alkyne) for the synthesis of solithromycin (**1**), we selected a small library of

**Table 1. Structures of (A) Alkyne Fragments in the Library and (B) Regioisomeric *anti* (1,4)- and *syn* (1,5)-Triazoles Derived from In Situ Click Experiments (R = Fragment)**

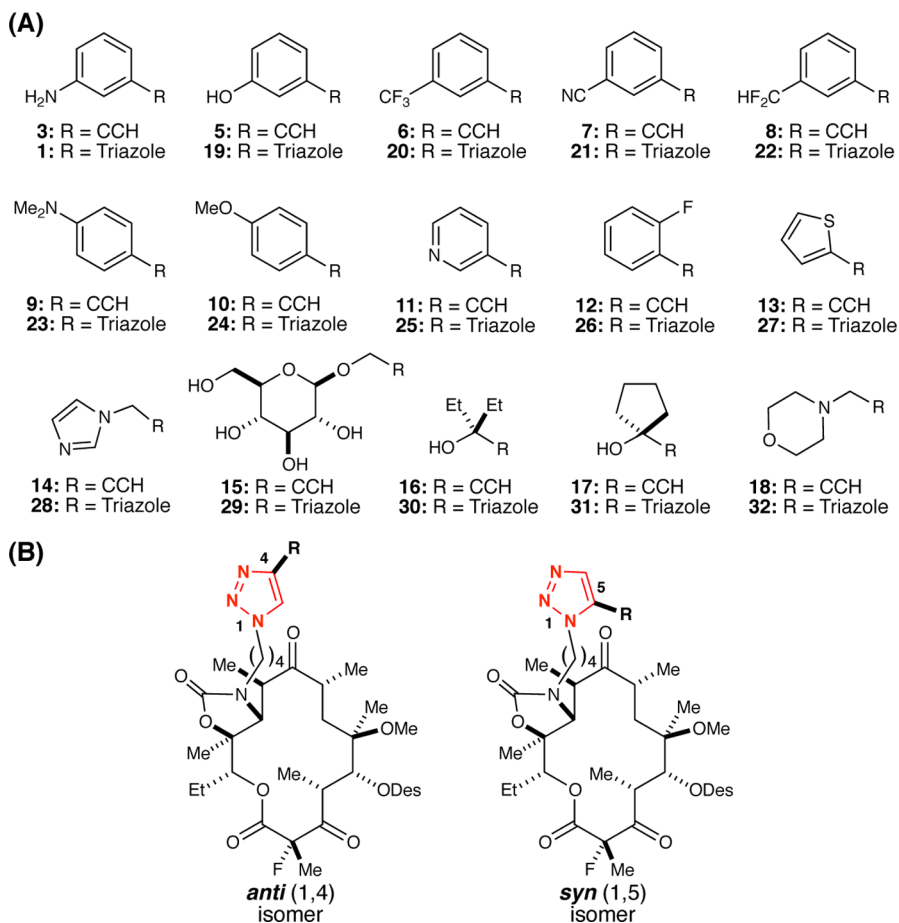


**Table 2.** Rank-Ordering of *anti*-Triazoles **1**, **19–32** and Azide Fragment **2** by Dissociation Constants ( $K_d$ ) for 70S *E. coli* Ribosomes Determined by Fluorescence Polarization, along with Experimental  $\Delta G$  Values (kcal/mol) and Calculated Normalized Ligand Grid Free Energies (LGFEs, kcal/mol) from SILCS<sup>a</sup>

compd	$K_d$ (nM)	$\Delta G$ (kcal/mol)	total LGFE (kcal/mol)	side-chain LGFE (kcal/mol)	Macro+Des LGFE (kcal/mol)
SOL ( <b>1</b> )	0.6 ± 0.1	-12.54	-49.67	-16.20	-35.38
<b>32</b>	0.8 ± 0.1	-12.41	-51.83	-17.09	-35.30
<b>19</b>	1.1 ± 0.1	-12.24	-48.72	-14.01	-35.33
<b>25</b>	1.1 ± 0.1	-12.22	-48.70	-14.87	-35.57
<b>23</b>	1.3 ± 0.2	-12.13	-52.16	-17.19	-34.27
<b>24</b>	1.4 ± 0.2	-12.06	-50.83	-15.50	-34.86
<b>28</b>	1.5 ± 0.1	-12.02	-47.80	-14.27	-35.83
<b>21</b>	1.6 ± 0.2	-12.00	-50.82	-16.23	-35.24
<b>22</b>	1.7 ± 0.2	-11.94	-52.61	-17.81	-35.08
<b>27</b>	1.8 ± 0.2	-11.91	-47.93	-13.64	-34.70
<b>Azide 2</b>	2.1 ± 0.4	-11.82	-38.85	-5.04	-35.85
<b>31</b>	2.4 ± 0.2	-11.74	-49.49	-15.15	-34.80
<b>30</b>	2.5 ± 0.3	-11.73	-48.96	-13.91	-35.37
<b>26</b>	2.5 ± 0.2	-11.72	-49.18	-15.39	-34.93
<b>20</b>	3.5 ± 0.5	-11.53	-52.86	-18.55	-34.91
<b>29</b>	5.0 ± 0.4	-11.32	-52.90	-18.10	-34.81
PI	N/A	N/A	-0.22	-0.14	0.37

<sup>a</sup>LGFEs are calculated for the total molecule, side-chain, and macrolactone+desosamine (Macro+Des) components. The side-chain is defined as the four-carbon alkyl linker and functionalized triazole extending from N11. Predictive indices (PIs) are calculated for each type of LGFE.<sup>45</sup>

structurally diverse alkynes for competition experiments (Table 1A). The library of 15 alkynes (Table 1A) contained both aromatic (e.g., **3**, **5–14**) and nonaromatic (e.g., **15–18**) functionalities, including 3-ethynylaniline (**3**) used in the synthesis of solithromycin (**1**). Aromatic alkynes were selected based on the potential to engage in  $\pi$ -stacking interactions with the 23S rRNA A752-U2609 Watson–Crick base-pair, and to allow assessment of the impact of a hydrogen bonding network established between the aniline in **1** and A752 (PDB 3ORB).<sup>13</sup> The nonaromatic alkynes included structural motifs that could bind rRNA via hydrogen bond donors (e.g., **15–17**), acceptors (e.g., **15–18**), or by forming electrostatic interactions (i.e., salt bridges) between the protonated amine in **32**, derived from morpholine **18**, and negatively charged phosphates. As shown in Figure 2, triazoles from the in situ click reaction with azide **2** and the alkynes (Table 1A) can yield *anti* (1,4)- and/or *syn* (1,5)-regioisomers, depending on the positioning of alkyne fragments that make optimal interactions with rRNA (Table 1B, represented as “R”).

Experiments were then undertaken to determine the ribosome binding affinity of azide **2** and the *anti* (1,4)-triazoles (Table 1B). To this end, *anti*-triazoles **1**, **19–32** were prepared by Cu(I)-catalysis as template-guided synthesis only provides analytically detectable quantities.<sup>40</sup> Products derived from the in situ click method are anticipated to possess greater target affinity, compared to the individual fragments, due to the additivity of binding energies (Scheme 1),<sup>14</sup> such that triazoles formed in the greatest amounts (i.e., highest mass counts) should possess higher affinity. To quantify binding affinity, dissociation constants ( $K_d$ ) of the *anti*-regioisomers of triazoles **1**, **19–32** and azide **2** for 70S *E. coli* ribosomes were measured by an established fluorescence polarization competition assay using BODIPY-functionalized erythromycin.<sup>11</sup> The results showed an 8-fold range of *anti*-triazole affinities, wherein **1**, **19**, **21–25**, **27–28**, and **32** bound more strongly than azide fragment **2** while *anti*-triazoles **20**, **26**, **29–31** were weaker binders than **2** (Table 2, Figure S1).

In order to rationalize the relatively narrow range of measured  $K_d$  values despite significant differences in the structures of the alkynes, we performed a computational analysis to understand the relative alkyne contributions to the binding affinities using the site-identification by ligand competitive saturation (SILCS) approach.<sup>41–44</sup> SILCS maps the functional group free energy affinity pattern of macromolecules onto a grid and may be used to quantitatively estimate relative binding affinities of ligands, yielding ligand grid free energies (LGFE). Details of the SILCS calculation and LGFE analysis are presented in the Supporting Information. Notably, the LGFE scores represent an atom-based free energy approximation allowing estimation of the contributions of different regions of molecules to binding affinity. Presented in Table 2 along with the experimentally determined  $K_d$  and  $\Delta G$  values ( $\Delta G = -RT \ln K_d$ ) are the calculated LGFE scores for *anti*-triazoles **1**, **19–32**, and azide **2**, including (1) the total LGFE score of each compound; (2) the LGFE contributions of the respective side-chains; and (3) the LGFE contributions of macrolactone and desosamine (Macro+Des) components. Analysis of the ability of the three LGFE metrics to predict the relative order of binding was then undertaken by calculating the predictive indices (PIs), which measures how well molecular modeling calculations track the ordering of the experimental binding values (see Supporting Information for details). The index varies from -1 (wrong prediction) to 0 (random) to +1 (perfect prediction).<sup>45</sup>

As shown in Table 2, the total and side-chain LGFE scores were not predictive whereas the Macro+Des LGFE yielded a satisfactory level of predictability. While somewhat unexpected, these results suggest that the binding of the ligands is dominated by the macrolactone and desosamine moieties, which are common to all of the triazole compounds. This hypothesis is consistent with the similarities in  $K_d$  values, with the relative binding affinities being associated with the ability of the unique side-chains to alter the interactions of the macrocycle and desosamine moieties with rRNA, rather than the side-chains directly interacting with rRNA themselves.



Further support is found in the relative binding of known ketolides in which the addition of a side-chain did not markedly increase efficacy. For example, clarithromycin—the precursor to telithromycin (**4**) and solithromycin (**1**)—has a  $K_d$  value of 1.7 nM despite the absence of a side-chain (see Supporting Information).<sup>11,13</sup> The significance and utility of the side-chains in congeners **1** and **4** is demonstrated by bacterial ribosomes that acquire resistance from either mutation or modification, which render first-generation antibiotics erythromycin and clarithromycin ineffective due to markedly decreased binding affinity.<sup>13,46,47</sup>

Detailed analysis revealed several important structure–activity relationships within the library. Specifically, *meta*- or 3-substituted aromatic and/or heteroaromatic groups with the ability to engage in hydrogen bonding provided the best boost in affinity relative to the azide alone (e.g., **1**, **19**, **21**–**22**, **25**). In contrast, the 3-substituted trifluoromethylphenyl, and 2-fluorophenyl triazoles, **20** and **26**, respectively, with no capacity for hydrogen bonding, failed to enhance affinity. In addition, the nonaromatic triazoles **29**, **30**, and **31** all showed decreased binding as compared to **2**, indicating that moieties that participate primarily in hydrogen bond interactions but cannot participate in  $\pi$ -stacking do not stabilize macrocycle+desosamine-rRNA interactions. These results suggest that the ability of the side-chain to participate in both  $\pi$ -stacking and hydrogen bonding leads to stabilization of macrocycle+desosamine-rRNA interactions. We attribute the relatively high binding activity of the nonaromatic morpholine-containing triazole **32**, which bound only slightly less tightly than solithromycin (**1**, SOL), to the presence of a basic amine that can interact electrostatically with rRNA. Lastly, the five-membered heteroaromatics **27**–**28** showed increased binding and thus represent an interesting, novel class to explore.

Guided by the  $K_d$  values, two in situ click experiments were designed wherein azide **2** was incubated with five different alkynes in the presence of 50S *E. coli* ribosomal subunits to test whether the target could differentiate between triazoles with  $K_d$  values lower than azide **2** and those with higher  $K_d$  values. The first experiment included 3-ethynylaniline (**3**), which is the precursor to solithromycin (**1**), along with **5**, **10**, **15**, and **16** (2 mM each; 10 mM total), 10  $\mu$ M azide **2**, and 10  $\mu$ M 50S *E. coli* ribosomal subunits at rt for 48 h. Azide and ribosomal subunit concentrations were doubled relative to the binary experiment to ensure sufficient product formation under competitive reaction conditions. The results (Figure 3) show that **1** provides the greatest combined mass counts, with the *anti*-regioisomer (solithromycin, **1**) being preferred over *syn*-**1**. Phenol-functionalized triazole **19**, which possessed a low  $K_d$  for the *anti*-regioisomer, was also formed in significant amounts. This fact establishes the importance of aromatic fragments with the capacity for hydrogen bonding with rRNA at the *meta*-position, again drawing an analogy to **1**. Triazole formation from glucosyl alkyne **15** resulted in small amounts of both *syn*- and *anti*-**29**. Aliphatic compound **30** was not formed in significant amounts, which we attribute to the absence of  $\pi$ -stacking interactions. Interestingly, triazole **24** was formed in the lowest amount, even though it is capable of  $\pi$ -stacking and has a  $K_d$  lower than that of azide **2**. We posit this phenomenon is most likely due to competitive product inhibition arising from **1** and **19**, which are two of the tightest binders in the library.<sup>14,21</sup>

The second, five-alkyne in situ click experiment featured alkynes bearing a range of functional groups such as alcohol **16**,

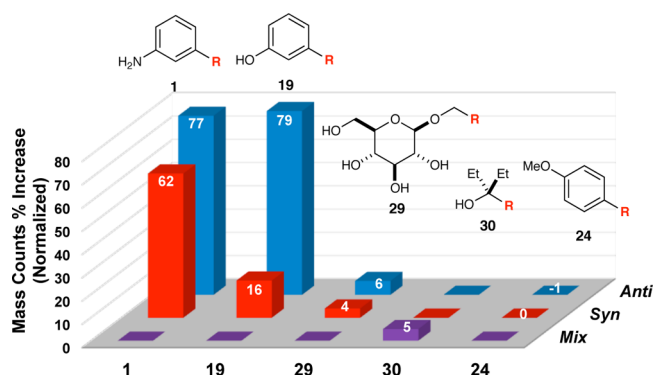


**Figure 3.** In situ click experiment with azide **2** and alkynes **3**, **5**, **10**, **15**, and **16**, yielding triazoles **1**, **19**, **24**, **29**, and **30**, respectively. Mix represents unresolved *anti*- and *syn*-isomers. Normalized mass count percent increases (provided in the bars) are calculated from the ratio of the ribosome-templated reaction to the background reaction. Results are an average of two experiments. The remainder of the molecule is abbreviated as “R”.

imidazole **14**, pyridine **11**, nitrile **7**, and fluoride **12**, selected to determine how the ribosome-templated reaction would perform in the presence of alkynes that yield triazoles binding more weakly than **1**. The results from the experiment are shown in Figure 4. Imidazole-functionalized triazole **28**, as a

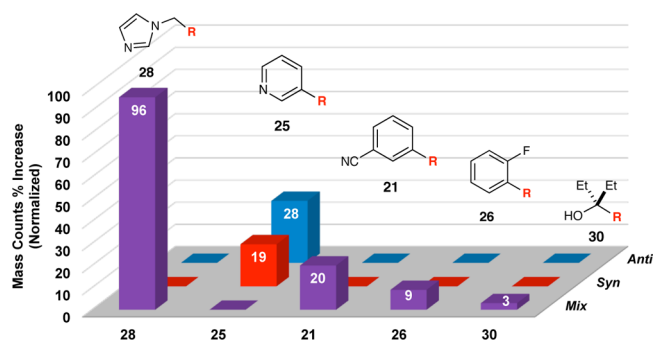


**Figure 4.** In situ click experiment with azide **2** and alkynes **7**, **11**–**12**, **14**, and **16** yielding triazoles **21**, **25**–**26**, **28**, and **30**, respectively. Mix represents unresolved *anti*- and *syn*-isomers. Normalized mass count percent increases (provided in the bars) are calculated from the ratio of the ribosome-templated reaction to the background reaction. Results are an average of two experiments. The remainder of the molecule is abbreviated as “R”.

mixture of *syn*- and *anti*-regioisomers, was detected in the greatest amount, consistent with the low  $K_d$  value for the *anti*-isomer, followed by **25** then **21**. In contrast, triazoles **26** and **30** were not detected in significant quantities. Taken together, the two five-alkyne in situ click experiments demonstrate that the ribosome can template the formation of tighter-binding triazoles in greater quantity.

The successful execution of five-alkyne in situ click experiments justified a greater exploration of chemical space while expanding the scope of the method. To this end, we initiated experiments with 15 alkynes, which would yield 30 congeners (Figure 5). These included alkynes from the two five-alkyne experiments, along with six additional alkynes (i.e., **6**, **8**–**9**, **13**, **17**–**18**). To ensure complete alkyne solubilization, the concentration of each member was decreased from 2 mM to 1 mM, and the concentrations of azide **2** and 70S *E. coli* ribosomes were maintained at 10  $\mu$ M each. The 15-component

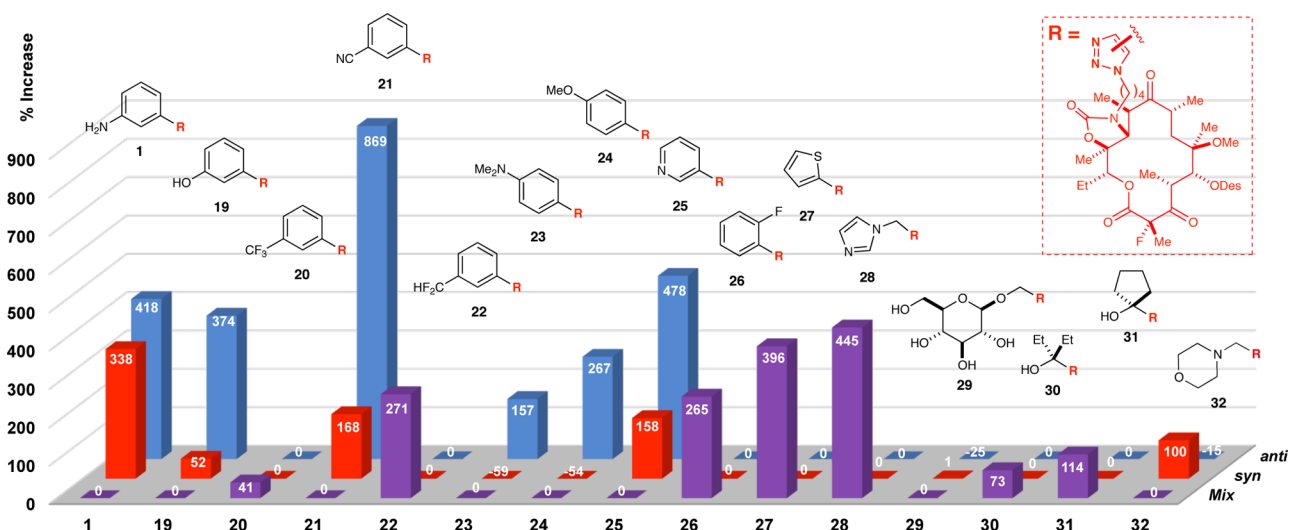


**Figure 5.** In situ click experiment with azide **2** and alkynes **3**, **5**–**18** yielding triazoles **1** and **19**–**32**, respectively. Mix represents an unresolved mixture of *anti*- and *syn*-isomers. Mass count percent increases (provided in the bars) are calculated from the ratio of the ribosome-templated reaction to the background reaction. Results are an average of five experiments.

**Table 3. Evaluation of Azide **2**, *anti*-Triazoles **1** (SOL) and **19**–**32** Using Minimum Inhibitory Concentration (MIC) Assays ( $\mu\text{g/mL}$ ) against *E. coli* and *S. pneumoniae* Strains<sup>a</sup>**

compd	$K_d$ (nM)	$\Delta G$ (kcal/mol)	MIC <i>E. coli</i> DK pKK 3535	MIC <i>E. coli</i> DK A2058G	MIC <i>S. pneumo</i> ATCC 49619	MIC <i>S. pneumo</i> 655 mefA
<b>27</b>	1.8	−11.9	1	1	0.004	0.5
<b>19</b>	1.1	−12.2	2	1	0.002	0.5
<b>28</b>	1.5	−12.0	2	2	0.032	4
SOL ( <b>1</b> )	0.6	−12.6	2	2	0.006	0.375
Azide <b>2</b>	2.1	−11.8	2	2	0.002	0.25
<b>24</b>	1.4	−12.1	2	2	0.005	1
<b>26</b>	2.5	−11.7	2	2	0.002	0.5
<b>25</b>	1.1	−12.2	2	2	0.016	0.5
<b>22</b>	1.7	−12.0	2	4	0.004	1
<b>23</b>	1.3	−12.1	4	4	0.008	1
<b>21</b>	1.6	−12.0	4	4	0.016	1
<b>31</b>	2.4	−11.7	4	4	0.016	2
<b>30</b>	2.5	−11.7	4	4	0.032	2
<b>20</b>	3.5	−11.5	4	4	0.016	2
<b>32</b>	0.8	−12.4	8	8	0.063	4
<b>29</b>	5	−11.3	>32	>32	4	>4
PI	N/A	N/A	0.46	0.48	0.34	0.44

<sup>a</sup>Compounds are rank-ordered by potency in MIC assays against *E. coli* and then *S. pneumoniae* strains. MIC values determined in three independent experiments; translation values in two independent experiments. Analysis of the data in this table reveals that the poorest-performing compounds (**32**, **20**, and **29**, shown in italics) against both strains correlate with the binding data; in fact, **20** and **29** had the highest  $K_d$  values. The polarity of **29** and **32** may be contributing to poor uptake and/or permeability. Predictive indices (PIs) are calculated for the MICs against each strain with respect to  $K_d$  values.

alkyne mixture (15 mM total) was sonicated for 1–5 min to obtain a homogeneous solution, prior to the addition of azide **2** and ribosomes, and the reaction mixture was incubated at rt for 48 h. Consistent with the five-alkyne in situ click reactions, we detected the formation of triazoles with  $K_d$  values lower than **2** (i.e., better binders than the azide fragment) including solithromycin (**1**), **19**, **21**–**25**, **27**, and **28** (Figure 5). All of these cycloadducts were derived from aromatic alkynes, again underscoring the significance of  $\pi$ -stacking interactions with the A752-U2609 base pair. The only aromatic triazole that was not detected in appreciable quantity was trifluoromethyl congener **20**. However, its  $K_d$  value (Table 2) was the second highest of the library, further illustrating selectivity in the in situ click process. Nonaromatic triazoles **29**, **30**, and **31** were not

detected in significant quantities. In addition, morpholine-functionalized **32** was not detected in significant quantities, despite the fact that it binds ribosomes as well as **1**. We attribute this observation to the basicity of *N*-propargyl morpholine (**18**), which, though its  $pK_a$  is 5.55,<sup>48</sup> could be protonated when bound to the ribosome due to electrostatic interactions with phosphate residues. Such binding could effectively sequester this fragment and preclude coupling with **2**. Competitive product inhibition, which was observed in both five-alkyne competition experiments (vide supra), may account for the modest formation of triazoles **20**, **29**–**32**.

Curiously, the ribosome-templated synthesis of solithromycin (**1**) gave slightly different *syn/anti* ratios for the binary reaction (~2:1) versus the five- and 15-alkyne competition

experiments, the latter two of which gave similar *syn/anti* ratios ( $\sim 1.24/1$ ). We also observed this reaction-dependent change in regioisomer ratios with phenol **19** and pyridine **25**. The isolation of nitrile **21** as a “mix” in Figure 4 and subsequent resolution thereof [i.e.,  $\sim 5:1$  (*anti/syn*)] in Figure 5 is attributed to chromatographic issues and not the reaction per se.<sup>49</sup> The modulation of regioisomer ratios illustrates the complex nature of in situ click competition experiments wherein the alkyne mixtures, which are in mM concentrations, are likely modifying the architecture of the macrolide-binding site via direct or allosteric interactions with rRNA. Finally, the marked and reproducible ribosome-templated formation of nitrile **21** in the 15-alkyne (Figure 5) vis-à-vis the five-alkyne experiment (Figure 4) is striking. This result is difficult to rationalize in terms of  $K_d$  or LGFE and may arise from the complexity of the reaction mixture. To probe this, we are currently investigating ten-alkyne mixtures that are more consistent with the prior art.<sup>20–25</sup>

We next assessed the mechanism of action of azide **2** and *anti*-triazoles **1**, **19–32** and evaluated their antibiotic activities using (1) in vitro protein synthesis assays using a cell-free system<sup>50</sup> and (2) minimum inhibitory concentration (MIC) assays for azide **2**, *anti*-triazoles **1**, and **19–32** (Table 3).<sup>51</sup> As the ribosome-templated in situ click process delivers bivalent inhibitors possessing greater potency than their monovalent components, it is important to determine the *selectivity* of the newly formed cycloadducts for bacterial versus mammalian ribosomes. To this end, we evaluated *anti*-triazoles **1** (solithromycin), azide **2**, and four analogues from our library using a mammalian cell toxicity assay with human fibroblasts.

For the in vitro translation inhibition studies, all of the compounds were assayed at 1  $\mu\text{M}$ . Given that the 70S concentration in the cell-free protein synthesis (CFPS) reactions are  $1.5 \pm 0.2 \mu\text{M}$  (RTS100 kit, SPRIME)<sup>50</sup> and  $1.4 \pm 0.1 \mu\text{M}$  (Expressway Mini kit, Invitrogen, see Supporting Information), we would expect these low- to sub- nM affinity compounds to bind 70S stoichiometrically, negating any differences in affinity and yielding an expected inhibition of approximately  $70 \pm 10\%$ . Indeed, all of the compounds, including the azide, inhibited the CFPS reaction in the range of  $48 \pm 16\%$  (see Supporting Information). This inhibition is toward the lower end of the predicted range, which may be due to inhibitor sequestration by other components in these heterogeneous lysate-based mixtures, reducing the effective inhibitor concentration. Differential sequestration between compounds could also explain the variation observed between the best inhibitor (**32**,  $64 \pm 14\%$  inhibition) and the worst inhibitor (**29**,  $32 \pm 5\%$  inhibition).

For the MIC assays, we tested solithromycin (**1**, SOL), azide **2**, and *anti*-triazoles **19–32** against various strains of *E. coli*, *S. pneumoniae*, and *S. aureus*.<sup>52</sup> Strains ATCC 29213 (*S. aureus*) and ATCC 49619 (*S. pneumoniae*) served as quality control strains with values for SOL (**1**), giving results closely matching published values.<sup>51</sup> The results in Table 3 show that thiophene-functionalized triazole **27** was 2-fold more potent than SOL against *E. coli* DK pkk3535 strain and A2058G strains and that the relatively high affinity (low  $K_d$ ) phenol-functionalized triazole **19** was 2-fold more potent than SOL in the *S. pneumoniae* ATCC wild-type and *E. coli* mutant DK A2058G strains.<sup>53</sup> Comprehensive structure–activity relationship studies of these two analogues could result in the discovery of novel, potent antibiotics. In addition, three of the poorest-performing compounds against both *S. pneumoniae* strains (**20**,

**29**, **30** shown in red) include two, **20** and **29**, having the highest  $K_d$  values. Consistent with this are the predictive indices (PIs) of the  $K_d$  values in Table 3 for the MIC values, indicating affinity to be a reasonable predictor of functional activity.<sup>45</sup> However, adduct **32** (also shown in red) is less potent than would be expected from its  $K_d$  value, which could indicate an uptake problem. Taken together, these results indicate satisfactory levels of selectivity in the ribosome-templated in situ click process. It is important to note that while solithromycin (**1**) and the library of analogues prepared herein maintained their efficacy against resistant *E. coli* and *S. pneumoniae* strains (Table 3), this was not the case for all resistant strains tested (see Tables S5 and S6, Supporting Information).

For the cell viability assays, the potential cytotoxicity of solithromycin (**1**), azide (**2**), and analogues **19**, **24**, **27**, and **28** against human dermal fibroblasts (GM05659, Coriell Institute, Camden, NJ)<sup>54</sup> was measured using a commercial luciferase-coupled ATP quantitation assay (CellTiter-Glo, Promega).<sup>55</sup> The cells were incubated with test compounds at concentrations ranging from 50  $\mu\text{M}$  to 0.88 nM for 24- and 48-h time periods (see Figures S3–S5, Supporting Information). Significantly, the data showed that, like **1**, compounds **24**, and **27–28** showed no effect on fibroblasts after 24 or 48 h up to low micromolar concentrations. The therapeutic indices for these compounds (i.e., bactericidal activity versus mammalian cytotoxicity) were essentially the same as that measured for solithromycin (**1**).

## CONCLUSION

We have developed an in situ click chemistry method that employs 70S *E. coli* ribosomes and 50S ribosomal subunits as platforms, with the ribosome-templated synthesis of solithromycin (**1**) serving as proof-of-concept. The method was applied in five- and 15-alkyne competition experiments. Consistent with other kinetic, target-guided in situ click processes, the extent of triazole formation correlated with ribosome binding affinity (see Chart S1, Supporting Information). The 50S *E. coli* ribosomal subunit was also studied using the computational site-identification by ligand competitive saturation (SILCS) approach. Interestingly, LGFEs associated with the macrolactone and desosamine moieties, rather than the full triazole structures, were correlated to dissociation constants for the congeners, suggesting that the side-chain indirectly impacts affinity by altering macrocycle–ribosome interaction.

The inclusion of bacterial ribosomes in the repertoire of targets represents a powerful drug discovery platform that obviates the onerous need to independently synthesize, characterize, and evaluate both *syn*- and *anti*-triazoles. Significantly, the use of ribosomes possessing known mechanisms of resistance (e.g., rRNA modification or mutation) can lead to the discovery of antibiotics that selectively target resistant over wild-type bacterial strains. Protein synthesis inhibition experiments confirmed the mechanism of action of these congeners. MIC evaluation of the in situ click products quantified antibiotic activity and firmly established this method as efficacious in the triaging and prioritization of potent antibiotic candidates targeting the bacterial ribosome. Finally, we showed that four analogues discovered using ribosome-templated in situ click chemistry (i.e., **19**, **24**, **27**, **28**) displayed similar therapeutic indices as that seen with solithromycin (**1**).



**■ ASSOCIATED CONTENT****■ Supporting Information**

The Supporting Information is available free of charge on the ACS Publications website at DOI: [10.1021/jacs.5b13008](https://doi.org/10.1021/jacs.5b13008).

General and in situ click methods and data, computational methods, determination of  $K_d$  by fluorescence polarization with BODIPY-labeled erythromycin, cell-free translation inhibition method and data, minimum inhibitory concentration (MIC) method and data, mammalian cell toxicity assay, synthetic methods including synthesis and full structural assignment of azide **2**, Cu(I)-catalyzed click synthesis and characterization of *anti*-triazoles **1**, **19–32**. (PDF)

**■ AUTHOR INFORMATION****Corresponding Author**

\*[randrade@temple.edu](mailto:randrade@temple.edu)

**Notes**

The authors declare the following competing financial interest(s): A.D.M. is cofounder and CSO of SilcsBio LLC.

**■ ACKNOWLEDGMENTS**

This work was supported by the NIH (AI080968, GM051501, and GM070855), the National Science Foundation Graduate Research Fellowship Program under Grant No. (DEG-12262) awarded to C.N.T., and the University of Maryland Computer-Aided Drug Design Center, and Temple University. We thank Prof. Paul Edelstein (Penn Medicine) for kindly providing us with wild-type and resistant *S. pneumoniae* strains. We thank Dr. Charles DeBrosse, Director of the NMR Facility at Temple Chemistry, for kind assistance with NMR experiments. Finally, we thank Dr. Charles W. Ross III for assistance with LC–MS experiments and for carefully reading this manuscript.

**■ REFERENCES**

- (1) Walsh, C. *Nat. Rev. Microbiol.* **2003**, *1*, 65.
- (2) Levy, S. B.; Marshall, B. *Nat. Med.* **2004**, *10*, S122.
- (3) Solomon, S. L.; Oliver, K. B. *Am. Fam. Physician* **2014**, *89*, 938.
- (4) Bush, K.; Courvalin, P.; Dantas, G.; Davies, J.; Eisenstein, B.; Huovinen, P.; Jacoby, G. A.; Kishony, R.; Kreiswirth, B. N.; Kutter, E.; Lerner, S. A.; Levy, S.; Lewis, K.; Lomovskaya, O.; Miller, J. H.; Mobashery, S.; Piddock, L. J. V.; Projan, S.; Thomas, C. M.; Tomasz, A.; Tulkens, P. M.; Walsh, T. R.; Watson, J. D.; Witkowski, J.; Witte, W.; Wright, G.; Yeh, P.; Zgurskaya, H. I. *Nat. Rev. Microbiol.* **2011**, *9*, 894.
- (5) Fox, J. L. *Nat. Biotechnol.* **2006**, *24*, 1521.
- (6) Wright, P. M.; Seiple, I. B.; Myers, A. G. *Angew. Chem., Int. Ed.* **2014**, *53*, 8840.
- (7) Humphrey, W.; Dalke, A.; Schulten, K. *J. Mol. Graphics* **1996**, *14*, 33.
- (8) Fernandes, P.; Pereira, D.; Jamieson, B.; Keedy, K. *Drugs Future* **2011**, *36*, 751.
- (9) Bryskier, A. *Clin. Microbiol. Infect.* **2000**, *6*, 661.
- (10) Tenson, T.; Mankin, A. *Mol. Microbiol.* **2006**, *59*, 1664.
- (11) Yan, K.; Hunt, E.; Berge, J.; May, E.; Copeland, R. A.; Gontarek, R. R. *Antimicrob. Agents Chemother.* **2005**, *49*, 3367.
- (12) Spahn, C. M. T.; Prescott, C. D. *J. Mol. Med.* **1996**, *74*, 423.
- (13) Llano-Sotelo, B.; Dunkle, J.; Klepacki, D.; Zhang, W.; Fernandes, P.; Cate, J. H. D.; Mankin, A. S. *Antimicrob. Agents Chemother.* **2010**, *54*, 4961.
- (14) Jencks, W. P. *Proc. Natl. Acad. Sci. U. S. A.* **1981**, *78*, 4046.
- (15) Mamidyal, S. K.; Finn, M. G. *Chem. Soc. Rev.* **2010**, *39*, 1252.
- (16) Rostovtsev, V. V.; Green, L. G.; Fokin, V. V.; Sharpless, K. B. *Angew. Chem., Int. Ed.* **2002**, *41*, 2596.
- (17) Boren, B. C.; Narayan, S.; Rasmussen, L. K.; Zhang, L.; Zhao, H. T.; Lin, Z. Y.; Jia, G. C.; Fokin, V. V. *J. Am. Chem. Soc.* **2008**, *130*, 8923.
- (18) Rees, D. C.; Congreve, M.; Murray, C. W.; Carr, R. *Nat. Rev. Drug Discovery* **2004**, *3*, 660.
- (19) Scott, D. E.; Coyne, A. G.; Hudson, S. A.; Abell, C. *Biochemistry* **2012**, *51*, 4990.
- (20) Manetsch, R.; Krasinski, A.; Radic, Z.; Raushel, J.; Taylor, P.; Sharpless, K. B.; Kolb, H. C. *J. Am. Chem. Soc.* **2004**, *126*, 12809.
- (21) Lewis, W. G.; Green, L. G.; Grynszpan, F.; Radic, Z.; Carlier, P. R.; Taylor, P.; Finn, M. G.; Sharpless, K. B. *Angew. Chem., Int. Ed.* **2002**, *41*, 1053.
- (22) Krasinski, A.; Radic, Z.; Manetsch, R.; Raushel, J.; Taylor, P.; Sharpless, K. B.; Kolb, H. C. *J. Am. Chem. Soc.* **2005**, *127*, 6686.
- (23) Grimster, N. P.; Stump, B.; Fotsing, J. R.; Weide, T.; Talley, T. T.; Yamauchi, J. G.; Nemezc, A.; Kim, C.; Ho, K. Y.; Sharpless, K. B.; Taylor, P.; Fokin, V. V. *J. Am. Chem. Soc.* **2012**, *134*, 6732.
- (24) Mocharla, V. P.; Colasson, B.; Lee, L. V.; Roper, S.; Sharpless, K. B.; Wong, C. H.; Kolb, H. C. *Angew. Chem., Int. Ed.* **2005**, *44*, 116.
- (25) Whiting, M.; Muldoon, J.; Lin, Y. C.; Silverman, S. M.; Lindstrom, W.; Olson, A. J.; Kolb, H. C.; Finn, M. G.; Sharpless, K. B.; Elder, J. H.; Fokin, V. V. *Angew. Chem., Int. Ed.* **2006**, *45*, 1435.
- (26) Hirose, T.; Sunazuka, T.; Sugawara, A.; Endo, A.; Iguchi, K.; Yamamoto, T.; Ui, H.; Shiomi, K.; Watanabe, T.; Sharpless, K. B.; Omura, S. *J. Antibiot.* **2009**, *62*, 277.
- (27) Namelikonda, N. K.; Manetsch, R. *Chem. Commun.* **2012**, *48*, 1526.
- (28) Poulin-Kerstien, A. T.; Dervan, P. B. *J. Am. Chem. Soc.* **2003**, *125*, 15811.
- (29) Sharpless, K. B.; Manetsch, R. *Expert Opin. Drug Discovery* **2006**, *1*, 525.
- (30) Willand, N.; Desroses, M.; Toto, P.; Dirie, B.; Lens, Z.; Villeret, V.; Rucktooa, P.; Loch, C.; Baulard, A.; Deprez, B. *ACS Chem. Biol.* **2010**, *5*, 1007.
- (31) Rzuczek, S. G.; Park, H.; Disney, M. D. *Angew. Chem., Int. Ed.* **2014**, *53*, 10956.
- (32) Millward, S. W.; Henning, R. K.; Kwong, G. A.; Pitram, S.; Agnew, H. D.; Deyle, K. M.; Nag, A.; Hein, J.; Lee, S. S.; Lim, J.; Pfeilsticker, J. A.; Sharpless, K. B.; Heath, J. R. *J. Am. Chem. Soc.* **2011**, *133*, 18280.
- (33) Agnew, H. D.; Rohde, R. D.; Millward, S. W.; Nag, A.; Yeo, W. S.; Hein, J. E.; Pitram, S. M.; Tariq, A. A.; Burns, V. M.; Krom, R. J.; Fokin, V. V.; Sharpless, K. B.; Heath, J. R. *Angew. Chem., Int. Ed.* **2009**, *48*, 4944.
- (34) Pfeilsticker, J. A.; Umeda, A.; Farrow, B.; Hsueh, C. L.; Deyle, K. M.; Kim, J. T.; Lai, B. T.; Heath, J. R. *PLoS One* **2013**, *8*, e76224.
- (35) Nag, A.; Das, S.; Yu, M. B.; Deyle, K. M.; Millward, S. W.; Heath, J. R. *Angew. Chem., Int. Ed.* **2013**, *52*, 13975.
- (36) Farrow, B.; Hong, S. A.; Romero, E. C.; Lai, B.; Coppock, M. B.; Deyle, K. M.; Finch, A. S.; Stratis-Cullum, D. N.; Agnew, H. D.; Yang, S.; Heath, J. R. *ACS Nano* **2013**, *7*, 9452.
- (37) Deyle, K. M.; Farrow, B.; Hee, Y. Q.; Work, J.; Wong, M.; Lai, B.; Umeda, A.; Millward, S. W.; Nag, A.; Das, S.; Heath, J. R. *Nat. Chem.* **2015**, *7*, 455.
- (38) Liang, C. H.; Yao, S. L.; Chiu, Y. H.; Leung, P. Y.; Robert, N.; Seddon, J.; Sears, P.; Hwang, C. K.; Ichikawa, Y.; Romero, A. *Bioorg. Med. Chem. Lett.* **2005**, *15*, 1307.
- (39) Grigoriadou, C.; Marzi, S.; Kirillov, S.; Gualerzi, C. O.; Cooperman, B. S. *J. Mol. Biol.* **2007**, *373*, 562.
- (40) Kolb, H. C.; Finn, M. G.; Sharpless, K. B. *Angew. Chem., Int. Ed.* **2001**, *40*, 2004.
- (41) Raman, E. P.; Yu, W.; Lakkaraju, S. K.; MacKerell, A. D., Jr. *J. Chem. Inf. Model.* **2013**, *53*, 3384.
- (42) Raman, E. P.; Yu, W.; Guvench, O.; Mackerell, A. D. *J. Chem. Inf. Model.* **2011**, *51*, 877.
- (43) Guvench, O.; MacKerell, A. D., Jr. *PLoS Comput. Biol.* **2009**, *5*, e1000435.



(44) Lakkaraju, S. K.; Yu, W.; Raman, E. P.; Hershfeld, A. V.; Fang, L.; Deshpande, D. A.; MacKerell, A. D., Jr. *J. Chem. Inf. Model.* **2015**, *55*, 700.

(45) Pearlman, D. A.; Charifson, P. S. *J. Med. Chem.* **2001**, *44*, 3417.

(46) Mankin, A. S. *Curr. Opin. Microbiol.* **2008**, *11*, 414.

(47) Dunkle, J. A.; Xiong, L.; Mankin, A. S.; Cate, J. H. D. *Proc. Natl. Acad. Sci. U. S. A.* **2010**, *107*, 17152.

(48) Williams, A.; Jencks, W. P. *J. Chem. Soc., Perkin Trans. 2* **1974**, 1760.

(49) The change in chromatographic separation of *syn/anti* regioisomers is a result of the reverse-phase HPLC columns, whose resolutions deteriorate with multiple passage of bacterial ribosomes or ribosomal subunits. We are working to ameliorate this issue.

(50) Rosenblum, G.; Chen, C.; Kaur, J.; Cui, X.; Goldman, Y. E.; Cooperman, B. S. *Nucleic Acids Res.* **2012**, *40*, e88.

(51) Reller, L. B.; Weinstein, M.; Jorgensen, J. H.; Ferraro, M. J. *Clin. Infect. Dis.* **2009**, *49*, 1749.

(52) See [Supporting Information](#) for MIC evaluation against a broader panel of wild-type and resistant strains of *E. coli*, *S. pneumoniae*, and *S. aureus*.

(53) DK/pKK3535 refer to a tolC(-) strain with wild-type (WT) ribosomes. DK/A2058G refer to a tolC(-) strain with a mixed population of WT and mutant ribosomes (ca. 1:1) wherein Adenine has mutated to Guanine, which represents a clinically significant mechanism of resistance. TolC is an outermembrane efflux pump that recognizes antibiotics (e.g., macrolides), thus making these tolC(-) *E. coli* DK strains useful (and relevant) models of pathogenic gram positive bacteria. Moreover, the ribosomes employed in this study are derived from *E. coli*.

(54) GM05659, *Fibroblast from Skin, Chest*; Coriell Institute for Medical Research: Camden, NJ; [https://catalog.coriell.org/0/Sections/Search/Sample\\_Detail.aspx?Ref=GM05659](https://catalog.coriell.org/0/Sections/Search/Sample_Detail.aspx?Ref=GM05659), accessed 2/10/16.

(55) *CellTiter-Glo Luminescent Cell Viability Assay*; Promega: Madison, WI; [https://www.promega.com/products/cell-health-and-metabolism/cell-viability-assays/celltiter\\_glo-luminescent-cell-viability-assay/](https://www.promega.com/products/cell-health-and-metabolism/cell-viability-assays/celltiter_glo-luminescent-cell-viability-assay/), accessed 2/10/16.